Accepted for Publication in the *Journal of Biological Physics*

Synchrotron-based Biological Microspectroscopy: From the Mid-Infrared through the Far-Infrared Regimes

L.M. Miller, G.D. Smith, and G.L. Carr

National Synchrotron Light Source, Brookhaven National Laboratory, Upton, NY 11973, USA

Short title: Synchrotron IR Biological Microspectroscopy

ABSTRACT

Infrared radiation from synchrotron storage rings serves as a high-brightness source for diffraction-limited microspectroscopy in both the mid- and far-infrared spectral ranges. Mid-infrared absorption, due to local vibrational modes within complex molecules, is shown to be sensitive to small chemical changes associated with certain diseases. Far-infrared modes are believed to result from the folding or twisting of larger, more complex molecules. The ability for the synchrotron source to perform microscopy at a frequency of 1 THz is demonstrated.

Keywords: biological microspectroscopy, far-infrared, mid-infrared, synchrotron radiation, THz microscopy.

Corresponding author(s): Lisa M. Miller, lmiller@bnl.gov; G.L. Carr, carr@bnl.gov

INTRODUCTION

Synchrotron radiation, the light produced by relativistic electrons in high-energy accelerators, extends from x-rays down through the infrared spectral range, and serves as a source for a number of biologically relevant measurement techniques. This is particularly true for the infrared where the high source brightness enables microspectroscopy to be performed at the unprecedented resolution of just a few microns, a size scale appropriate for investigating individual cells. This is a significant capability, since biological cells and tissues are extremely complex structures that vary widely in composition. For nearly 20 years, infrared microspectroscopy (IRMS) has been used as a probe of sample biochemistry. This is due to the fact that infrared (IR) light excites molecular vibrations, where the frequency of each vibration is dependent upon the chemical structure of the molecule. For example, lipids have long hydrocarbon chains, so the dominant features in the IR spectrum of lipids are attributed to the asymmetric and symmetric stretching vibrations of CH_3 (2956 and 2874 cm^{-1}) and CH_2 (2922 and 2852 cm^{-1}) groups in the molecule (Figure 1). Other biological components, such as proteins, nucleic acids, and carbohydrates, also have unique IR spectra. The protein spectrum has two primary features, the Amide I (1600-1700 cm^{-1}) and Amide II (1500-1560 cm^{-1}) bands, which arise from specific stretching and bending vibrations of the peptide backbone. The frequency of the Amide I band is particularly sensitive to protein secondary structure. The nucleic acid spectrum has unique features in the region between 1000-1500 cm^{-1} that arise from asymmetric (1224 cm^{-1}) and symmetric (1087 cm^{-1}) phosphate stretching vibrations.

The assignments of various spectral features in biological samples have been the subject of numerous publications, which have been reviewed recently [1]. However, it should be

emphasized that these frequencies are offered as guidelines only, and that the recipe for assignment of IR absorption features in biological samples requires knowledge of both sample histology and pathology, in addition to spectroscopy. Armed with this information, variations in nucleic acid, protein, and lipid content or structure, can provide important details about the chemistry of diseased states. For example, aggregates of misfolded proteins, i.e. amyloid plaques, have been identified in the brain tissue of Alzheimer's disease patients [2,3]. Spectral evidence of cervical cancer [4,5], heart disease [6] and bone diseases such as osteoarthritis, osteoporosis, and osteogenesis imperfecta [7-12] have been identified. In addition, contaminants in human tissue, such as silicone in breast tissue [13] and narcotic metabolites in human hair [14-16] have also been observed.

Although conventional IR microspectroscopy has proven extremely valuable for resolving the chemical components in biological samples, the long wavelengths of IR radiation limit the spatial resolution that can be achieved. When considering the available spatial resolution, two issues should be taken into account. The first consideration is the acceptable signal-to-noise ratio (S/N), which decreases as apertures are closed to confine the IR beam to smaller areas. The second issue is diffraction. Existing instruments using a conventional IR source encounter a S/N limitation when apertures confine the IR to an area of 20-30 μm in diameter. This constrains the analysis of biological specimens to the tissue level only. Individual biological cells are typically 5-30 μm in diameter, making them too small to probe with a conventional IR source.

The high brightness of the synchrotron source (defined as the photon flux or power emitted per source area and solid angle) allows smaller regions to be probed with acceptable S/N [17,18]. This brightness advantage is not because the synchrotron produces more power, but rather

because the effective source size is small and the light is emitted into a narrow range of angles. Using a synchrotron source, aperture settings smaller than the wavelength of light can be used; though in this case, diffraction controls the available spatial resolution [19,20]. Thus for a typical biological specimen, the diffraction-limited spatial resolution for primary lipid (C-H stretch), protein (Amide I), and nucleic acid (P-O stretch) absorption features is approximately 3, 6, and 12 μm, respectively. The improvement in spatial resolution achieved by using a synchrotron IR source has only been realized recently, and its application to biological systems is still in its infancy.

APPLICATIONS

The high spatial resolution of a synchrotron IR source permits the chemical mapping of single living cells for the first time. Individual mouse hybridoma B cells have been examined during necrosis and also during the cell cycle and end phases of mitosis [21-23]. In these experiments, cells were deposited onto BaF_2 disks. This technique removes excess solution while keeping the cells sufficiently hydrated that they remain alive for several hours. IR maps are collected during this time by automated raster-scanning of the sample. The synchrotron infrared light does not cause heating or cytotoxic effects [24,25], but the cells eventually dehydrate and begin to die after about 8 hours [22].

With the ability to probe smaller and smaller areas with the synchrotron IR microscope, new techniques are currently being applied to aid in sample visualization. For example, an infrared microscope has recently been modified to perform simultaneous fluorescence microscopy and IRMS [26,27]. This technique has recently been applied to osteoporosis, where 5 μm-wide

layers of newly deposited bone have been examined [10,12]. In these studies, monkeys were administered different fluorochrome labels at one or two time points after removal of their ovaries; these labels are taken up into regions of new bone formation. By combining fluorescence microscopy (to identify new bone) and synchrotron IRMS, the chemical composition of newly remodeled bone was compared at various time points after ovariectomy. Results suggested that ovariectomy results in a reduced rate of bone mineralization and that treatment with nandrolone decanoate, an anabolic steroid, changes the composition of newly remodeled bone.

On the cellular and sub-cellular level, fluorescence microscopy can be used to visualize fluorescent tags bound to particular cellular components and even antibodies to individual proteins. Once identified, the IR microscope can be used to analyze the chemical environment in and around that region of interest. It should be noted that fluorescent labels are generally present in extremely low (i.e. nanomolar) concentrations, so they do not interfere with the IR technique; they are used exclusively for visualizing a region of interest. As an example, different fluorochrome labels were used to identify early and late stages of apoptosis, i.e. programmed cell death, in single mouse Jurkat cells, while synchrotron IRMS is used to examine chemical changes throughout the process [28]. Apoptosis was induced by using an anti-Fas monoclonal antibody and a Fas-positive Jurkat cell line. With this system, the kinetics of apoptosis can be controlled. Evidence of protein phosphorylation and/or nucleic acid degradation were evident in early apoptosis, where protein aggregation and degradation were not observed until the very late stages of the process.

Infrared spectroscopy is a valuable technique for studying protein structure by examination of the Amide I absorption band (1600 – 1700 cm^{-1}). A number of diseases are characterized by the formation of aberrant protein structure, i.e. protein misfolding. Synchrotron IRMS has been used to examine this process in Alzheimer's disease, where the brain is characterized by the presence of misfolded protein aggregates (β-amyloid plaques) that are thought to kill neurons in the brain [2,3,28]. In the study by Miller, *et al*., the β-amyloid plaques were fluorescently labeled with Thioflavin S. By combining fluorescence microscopy and synchrotron IRMS, the plaques were identified in the tissue and the *in situ* structure of the misfolded β-amyloid protein was determined (Figure 2). Results showed that the Amide I band of the amyloid plaque contains two peaks, indicating a mixture of secondary structures in the plaque region. In addition to the typical α-helical component near 1650 cm^{-1}, an intense second peak was apparent near 1630 cm^{-1}, which is indicative of a β-sheet protein structure. Thus, the formation of β-amyloid plaque in the brain is associated with a change in protein secondary structure from α-helical to β-sheet, which likely leads to aggregation of the misfolded protein.

RECENT DEVELOPMENTS

When the requirement for spatial resolution can be relaxed to ~ 100 microns or larger, far-infrared microspectroscopy becomes a feasible tool for studying biological materials. Less is know about the vibrational spectra of complex molecules in this spectral range, but it has been suggested that some low frequency modes are related to protein folding, while others correspond to twisting modes of DNA molecules. It is not our present goal to address directly these problems, but merely to point out the value of the synchrotron source for exploring small specimens in this spectral range. The source's high brightness extends into the far-infrared and

THz spectral range, enabling microspectroscopy of diffraction-limited areas to frequencies as low as 20 cm^{-1} (i.e., below 1 THz). Though the limit on spatial resolution is far larger (typically 100 microns in diameter) than for the mid-IR, the spectral range is of interest due to the variety of low frequency modes expected for large complex molecules such as proteins [29] and nucleic acids [30] [31,32]. For this purpose, we have modified a conventional mid-IR microscope system to open this spectral range for the purpose of "THz microspectroscopy". Two types of modifications were made to a Spectra-Tech "Irμs". First, the conventional Ge on KBr mid-IR beamsplitter was replaced with a custom "solid substrate" type beamsplitter (provided by Thermo Nicolet Corp.). Second, the optical beam path and the electronics were modified for an external ℓHe cooled bolometer (far-infrared detector). The new beamsplitter, though intended for use only below 700 cm^{-1}, provides significant interferometric modulation to several thousand wavenumbers when accurately aligned, and spectra up to 4000 cm^{-1} can still be obtained with the system. The interference fringes that result from this type of beamsplitter (~1 cm^{-1} perdiodicity) are not resolved with this particular microspectrometer. To accommodate an external detector, a special beam "port" was added to the microspectrometer purge enclosure. A switchable internal mirror, designed to intercept the collimated beam just upstream of the system's conventional mid-IR MCT detector, directs the infrared out through the new port and on to an off-axis paraboloidal mirror that focuses the light into the bolometer. The bolometer is a standard configuration for far-infrared, rapid scan FTIR spectroscopy, supplied by Infrared Laboratories. Two long-pass filters can be selected to optimize the signal-to-noise for either the 600 cm^{-1} to 50 cm^{-1} or the 100 cm^{-1} to <20 cm^{-1} spectral ranges. No special modifications were made to the detector for the purpose of microspectroscopy.

As anticipated, better long wavelength performance was achieved with the microscope's 15X, 0.58NA Schwarszchild objective than with its 32X, 0.67NA Schwarszchild objective. This was expected based on the larger diameter (about 14mm) entrance pupil of the 15X objective, which is approximately twice that of the 32X. The upstream optical system delivers the light to either objective through an intermediate aperture (the "upper aperture", see Figure 3). The NA for this part of the system is about 0.04, so the minimum spotsize at the intermediate focus is 25 times the wavelength. For a very far-infrared wavelength of 400 μm (frequency of 25 cm^{-1}), the spotsize at this focus is 10 mm, and already larger than the entrance pupil of the 32X objective (which, to make matters worse, is located about 180 mm downstream of this intermediate focus position). The larger entrance pupil of the 15X will capture more of this long wavelength light to deliver better performance. Even better performance would be expected from an objective with a larger entrance pupil.

To demonstrate the available signal-to-noise, we have collected consecutive "single-beam" spectra and ratioed them to yield "100% lines", with deviations from unity indicating the signal-to-noise. Two such 100% lines are shown in Figure 4, one for 100 μm confocal apertures (spectral range above 100 cm^{-1}) and the other for 500 μm confocal apertures (spectral range below 100 cm^{-1}) . We observe that the measurement noise is typically much less than 1%.

As another demonstration of the spectrophotometric accuracy of the instrument, we measured the reflectance of a KCl substrate (a conventional window material for mid-IR spectroscopy). The far-infrared properties of KCl are dominated by a strong phonon mode at 142 cm^{-1} (S=2.3) and weaker modes at 190 and 212 cm^{-1}. The measured reflectance for such a KCl substrate is shown in Figure 5, along with a calculated fit based on 3 Lorentzian oscillators to account for the

phonon modes. The fits yielded mode frequencies are 141.8 cm^{-1}, 189.5 cm^{-1}, and 211.6 cm^{-1}, which are within 0.5% of the known values.

As our last example, we have measured the transmission through a < 1 mm diameter sample of DNA. For the measurement, a small piece of dried fibrous salmon testes DNA was pressed between diamond substrates until the material turned clear, suggesting we had removed most of the voids (at least those larger than a few hundred nanometers). The resulting thin section (between 50 and 100 microns thick) was left attached to one of the diamonds, which then served as a transparent substrate. Transmission measurements were performed using the bare diamond as a reference, and the results converted to an absorption coefficient (assuming negligible effects due to reflection). The results are shown in Figure 6, and are remarkably similar to the recent results of Globus *et al* [32].

SUMMARY AND OUTLOOK

The high brightness of the synchrotron IR source has opened the door to cellular and sub-cellular chemical imaging of living cells. With enhanced visualization techniques, sub-cellular components can be investigated. Moreover, the combination of high spatial resolution with excellent S/N permits the examination of ongoing cellular processes in real-time. This high brightness extends into the THz spectral range, and THz microspectroscopy has been demonstrated for a number of standard specimens. We expect this capability will be useful for the study of complex biological molecules, as part of a research program to identify and understand the interaction of THz radiation with biological tissues.

In addition to microspectroscopic imaging, methods for studying protein folding and reaction dynamics on a sub-millisecond time scale are also being developed through the use of a unique rapid-mix IR flow cell [33]. Time-dependent phenomena can be probed on even shorter (i.e. sub-nanosecond) time scales by taking advantage of the pulsed nature of the synchrotron source [20]. No other pulsed IR source spans the large spectral range produced by a synchrotron. In addition, significant flux in the far-IR region continues to prove useful for the analysis of low frequency, collective modes in proteins[29]. Microspectroscopy in the far-IR spectral range has recently been demonstrated [34], and here we show its extension to frequencies below 1 THz.

The pursuit of improved spatial resolution with the synchrotron IR source will continue, based on both conventional (far-field) and possibly near-field techniques. For example, increasing the optical system numerical aperture by "immersing" the specimen in a high index material (e.g. KRS-5, ZnSe, germanium) can lead to factors of two or higher improvements in the spatial resolution. In a related technique, germanium planar waveguide technology has been used to isolate single Xenopus laevis oocytes membranes and identify protein and lipid components [35]. Near field techniques, where a small (sub-micron) source of IR is scanned very near to the specimen, have been demonstrated with IR laser sources[36,37], and similar technology may be applicable to synchrotron radiation microspectroscopy as well.

ACKNOWLEDGEMENTS

Portions of this work were funded through Laboratory Directed Research and Development (LDRD) funds at Brookhaven National Laboratory. The National Synchrotron Light Source is supported by the United States Department of Energy under contracts DE-AC02-98CH10886 and DE-AC05-84ER40150, respectively.

REFERENCES

1 Jackson, M., Mantsch, H.H., Encyclopedia of Analytical Chemistry. Wiley & Sons, Chichester, Sussex, UK, 2000.

2 Choo, L.P., Mansfield, J.R., Pizzi, M., Somorjai, R.L., Jackson, M., Halliday, W.C., Mantsch, H.H.: "Infrared spectra of human central nervous system tissue: diagnosis of Alzheimer's disease by multivariate analyses", Biospectroscopy, 1 (1995), 141-48.

3 Choo, L.P., Wetzel, D.L., Halliday, W.C., Jackson, M., LeVine, S.M., Mantsch, H.H.: "In situ characterization of beta-amyloid in Alzheimer's diseased tissue by synchrotron Fourier transform infrared microspectroscopy", Biophys J, 71 (1996), 1672-9.

4 Chiriboga, L., Xie, P., Yee, H., Zarou, D., Zakim, D., Diem, M.: "Infrared spectroscopy of human tissue. IV. Detection of dysplastic and neoplastic changes of human cervical tissue via infrared microscopy", Cell Mol Biol (Noisy-le-grand), 44 (1998), 219-29.

5 Lowry, S.R.: "The analysis of exfoliated cervical cells by infrared microscopy", Cell Mol Biol (Noisy-le-grand), 44 (1998), 169-77.

6 Liu, K.Z., Dixon, I.M., Mantsch, H.H.: "Distribution of collagen deposition in cardiomyopathic hamster hearts determined by infrared microscopy [In Process Citation]", Cardiovasc Pathol, 8 (1999), 41-7.

7 Paschalis, E.P., Jacenko, O., Olsen, B., deCrombrugghe, B., Boskey, A.L.: "The role of type X collagen in endochondral ossification as deduced by Fourier transform infrared microscopy analysis", Connect Tissue Res, 35 (1996), 371-7.

8 Camacho, N.P., Landis, W.J., Boskey, A.L.: "Mineral changes in a mouse model of osteogenesis imperfecta detected by Fourier transform infrared microscopy", Connect Tissue Res, 35 (1996), 259-65.

9 Miller, L.M., Hamerman, D., Chance, M.R., Carlson, C.S.: "Chemical Differences in Subchondral Osteoarthritic Bone Observed with Synchrotron Infrared Microspectroscopy", SPIE, 3775 (1999), 104-12.

10 Miller, L.M., Tibrewala, J., Carlson, C.S.: "Examination of Bone Chemical Composition in Osteoporosis Using Fluorescence-Assisted Synchrotron Infrared Microspectroscopy", Cellular and Molec. Biol., 46 (2000), 1035-44.

11 Miller, L.M., Vairavamurthy, V., Chance, M.R., Paschalis, E.P., Betts, F., Boskey, A.L., Mendelsohn, R.: " *In Situ* Analysis of Mineral Crystallinity and Environment in Bone using Infrared Microspectroscopy", Biochim. Biophys. Acta, 1527 (2000).

12 Huang, R., Miller, L.M., Carlson, C.S., Chance, M.R.: "FTIR Analysis of Tibia Bone From Ovariectomized Cynomolgus Monke*ys (Macaca fascicala*ris) and the Effect of Nandrolone Decanoate Treatment", Bone, 30 (2002), in press.

13 Ali, S.R., Johnson, F.B., Luke, J.L., Kalasinsky, V.F.: "Characterization of silicone breast implant biopsies by Fourier transform infrared mapping", Cell Mol Biol (Noisy-le-grand), 44 (1998), 75-80.

14 Kalasinsky, K.S., Magluilo, J., Jr., Schaefer, T.: "Hair analysis by infrared microscopy for drugs of abuse", Forensic Sci Int, 63 (1993), 253-60.

15 Kalasinsky, K.S., Magluilo, J., Jr., Schaefer, T.: "Study of drug distribution in hair by infrared microscopy visualization", J Anal Toxicol, 18 (1994), 337-41.

16 Kalasinsky, K.S.: "Drug distribution in human hair by infrared microscopy", Cell Mol Biol (Noisy-le-grand), 44 (1998), 81-7.

17 Carr, G.L., Reffner, J.A., Williams, G.P.: "Performance of an infrared microspectrometer at the NSLS", Rev. Sci. Instr., 66 (1995), 1490-92.

18 Reffner, J.A., Martoglio, P.A., Williams, G.P.: "Fourier Transform Infrared Microscopical Analysis with Synchrotron Radiation: The Microscope Optics and System Performance", Rev. Sci. Instr., 66 (1995), 1298.

19 Carr, G.L., Williams, G.P.: "Infrared microspectroscopy with synchrotron radiation", SPIE Conf. Proc., 3153 (1997), 51-59.

20 Carr, G.L.: "High-resolution microspectroscopy and sub-nanosecond time-resolved spectroscopy with the synchrotron infrared source", Vibrational Spectroscopy, 19 (1999), 53-60.

21 Jamin, N., Dumas, P., Moncuit, J., Fridman, W.H., Teillaud, J.L., Carr, G.L., Williams, G.P.: "Chemical imaging of nucleic acids, proteins and lipids of a single living cell. Application of synchrotron infrared microspectrometry in cell biology", Cell Mol Biol (Noisy-le-grand), 44 (1998), 9-13.

22 Jamin, N., Dumas, P., Moncuit, J., Fridman, W.H., Teillaud, J.L., Carr, G.L., Williams, G.P.: "Highly resolved chemical imaging of living cells by using synchrotron infrared microspectrometry", Proc Natl Acad Sci U S A, 95 (1998), 4837-40.

23 Holman, H.Y., Martin, M.C., Blakely, E.A., Bjornstad, K., McKinney, W.R.: "IR spectroscopic characteristics of cell cycle and cell death probed by synchrotron radiation based Fourier transform IR spectromicroscopy", Biopolymers, 57 (2000), 329-35.

24 Martin, M.C., Tsvetkova, N.M., Crowe, J.H., McKinney, W.R.: "Negligible sample heating from synchrotron infrared beam", Applied Spectr., 55 (2001), 111-13.

25 Holman, H.Y., Bjornstad, K.A., McNamara, M.P., Martin, M.C., McKinney, W.R., Blakely, E.A.: "Synchrotron infrared spectromicroscopy as a novel bioanalytical microprobe for individual living cells: cytotoxicity considerations", J Biomed Opt, 7 (2002), 417-24.

26 Tague, T., Miller, L.M.: "Novel use of fluorescence illumination with an infrared microscope", Microscopy Today, 2 (2000).

27 Miller, L.M., Tague, T.J.: "Development and biomedical applications of fluorescence-assisted synchrotron infrared micro-spectroscopy", Vibrational Spectroscopy, 849 (2002), 1-7.

28 Miller, L.M., Dumas, P., Jamin, N., Teillaud, J.-L., Miklossy, J., Forro, L.: "Combining IR spectroscopy and fluorescence imaging in a single microscope: Biomedical applications using a synchrotron infrared source", Rev. Sci. Instr., 73 (2002), 1357-60.

29 Xie, A., He, Q., Miller, L.M., Sclavi, B., Chance, M.R.: "Low frequency vibrations of amino acid homo-polymers observed by synchrotron far infrared absorption spectroscopy: Excited state affects dominate the temperature dependence of the spectra", Biopolymers, 49 (1999), 591-603.

30 Wittlin, A., L. Genzel, Kremer, F., Häseler, S., Poglitsch, A., Rupprecht, A.: "Far-infrared spectroscopy on oriented films of dry and hydrated DNA", Phys. Rev. A, 34 (1986), 493-500.

31 Markelz, A.G., Roitberg, A., Heilweil, E.J.: "Pulsed terahertz spectroscopy of DNA, bovine serum albumin and collagen between 0.1 and 2.0 THz", Chem. Phys. Lett., 320 (2000), 42-48.

32 Globus, T.R., Woolard, D.L., Samuels, A.C., Gelmont, B.L., Hesler, J., Crowe, T.W., Bykhovskaia, M.: "Submillimeter-wave Fourier transform spectroscopy of biological macromolecules", J. Appl. Phys., 91 (2002), 6105-15.

33 Marinkovic, N.S., Adzic, A.R., Sullivan, M., Kovacs, K., Miller, L.M., Rousseau, D.L., Yeh, S.R., Chance, M.R.: "Design and implementation of a rapid-mix flow cell for time-resolved infrared microspectroscopy", Rev. Sci. Instr., 71 (2000), 4057-60.

34 Miller, L.M., Sullivan, M., Toomey, J., Marinkovic, N., Carr, G.L., Williams, G.P., Chance, M.R.: "Biological Infrared Microspectroscopy at the National Synchrotron Light Source", Synchr. Rad. Instr.. 521 (1999), 47-50.

35 Plunkett, S.E., Jonas, R.E., Braiman, M.S.: "Vibrational spectra of individual millimeter-size membrane patches using miniature infrared waveguides", Biophys J, 73 (1997), 2235-40.

36 Palanker, D.V., Knippels, G.H., Smith, T.I., Swettman, H.A.: "IR microscopy with a transient photo-induced near-field probe (tipless near-field microscopy) "Optics Commun., 148 (1998), 215-20.

37 Knoll, B., Keilmann, F.: "Near-field probing of vibrational absorption for chemical microscopy" Nature, 399 (1999), 134.

FIGURE CAPTIONS

1. Various cellular components have dramatically different IR spectra as demonstrated by IR spectra of **(A)** a lipid (palmitic acid), **(B)** a protein (myoglobin), **(C)** a poly-nucleic acid, and **(D)** a carbohydrate (sucrose). For all spectra, films were prepared on BaF_2 disks and 128 scans were collected at 4 cm^{-1} resolution using a globar source.

2. **(A)** Optical image of an Alzheimer's diseased brain section under normal illumination and **(B)** fluorescence illumination using the Continuμm IR microscope (320x magnification). **(C)** Infrared micro-spectra of healthy brain tissue (dark area indicated by lower square in **(B)**) and amyloid deposits in the blood vessel walls (light area indicated by upper square in **(B)**). Data were collected using a 10 x 10 μm square aperture, 128 scans/point, at 4 cm^{-1} resolution.

3. Schematic of the Spectra-Tech *Irμs*™ scanning infrared microspectrometer used for this study. The system is a combined FTIR spectrometer and microscope, with an upper aperture to define the area being illuminated by the IR, and a lower aperture to limit the detector's field of view onto the sample. The term "confocal" is often used to describe the optical configuration when both apertures are used.

4. A "100% line", demonstrating the signal-to-noise for the far-infrared microspectrometer system using the synchrotron source. *Solid circles* - THz range using 500μm confocal apertures. *Open circles* - far-infrared range with 100μm confocal apertures. Each scan was acquired in about 2 minutes, and at a spectral resolution of 4 cm^{-1}.

5. Example far-infrared reflectance spectrum obtained for a KCl crystalline substrate, along with a fit based on 3 Lorentzian oscillators.

6. Microscopy measurement of the far-infrared absorption coefficient for a thin section of salmon DNA.

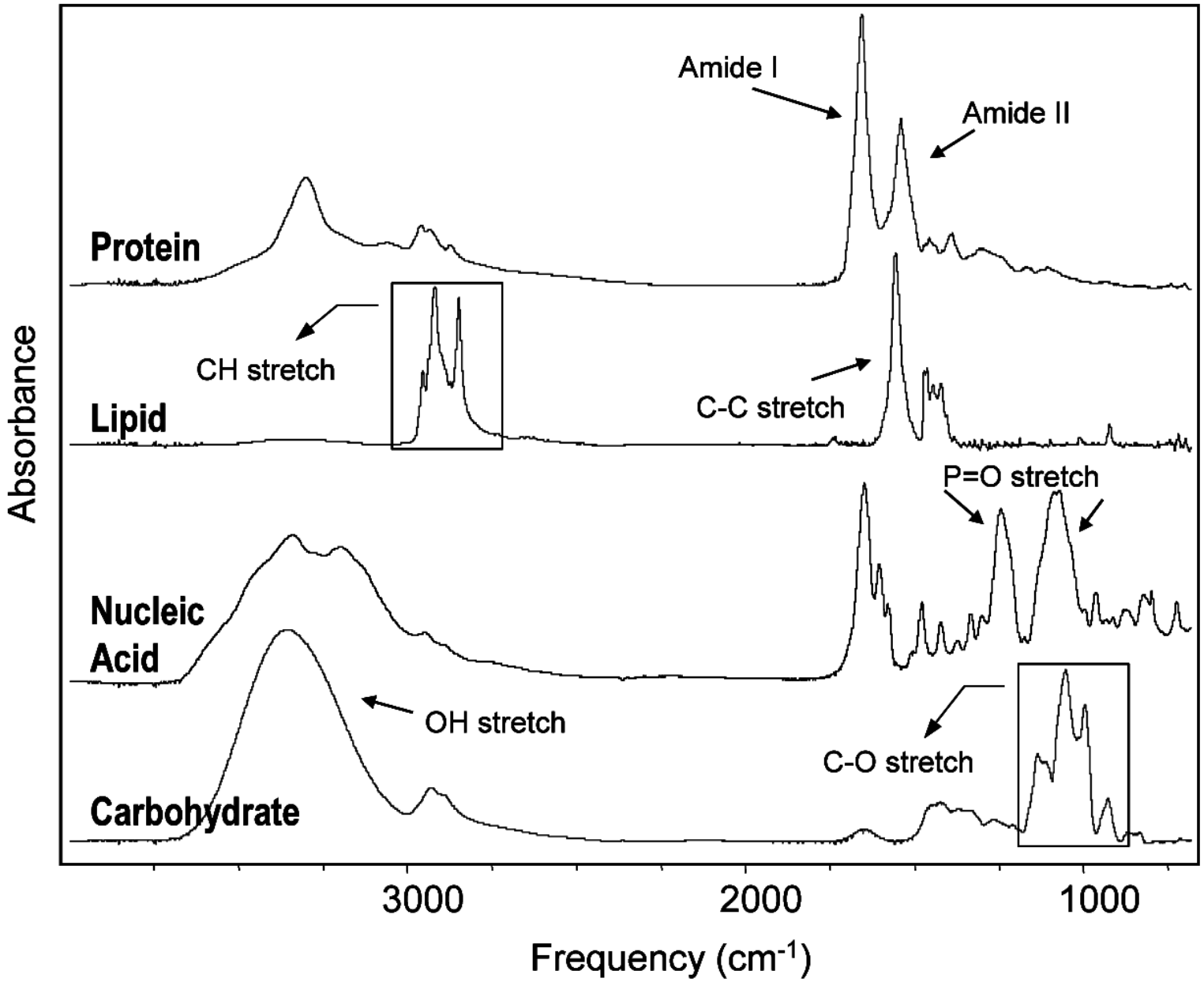

L.M. Miller et al Figure 1

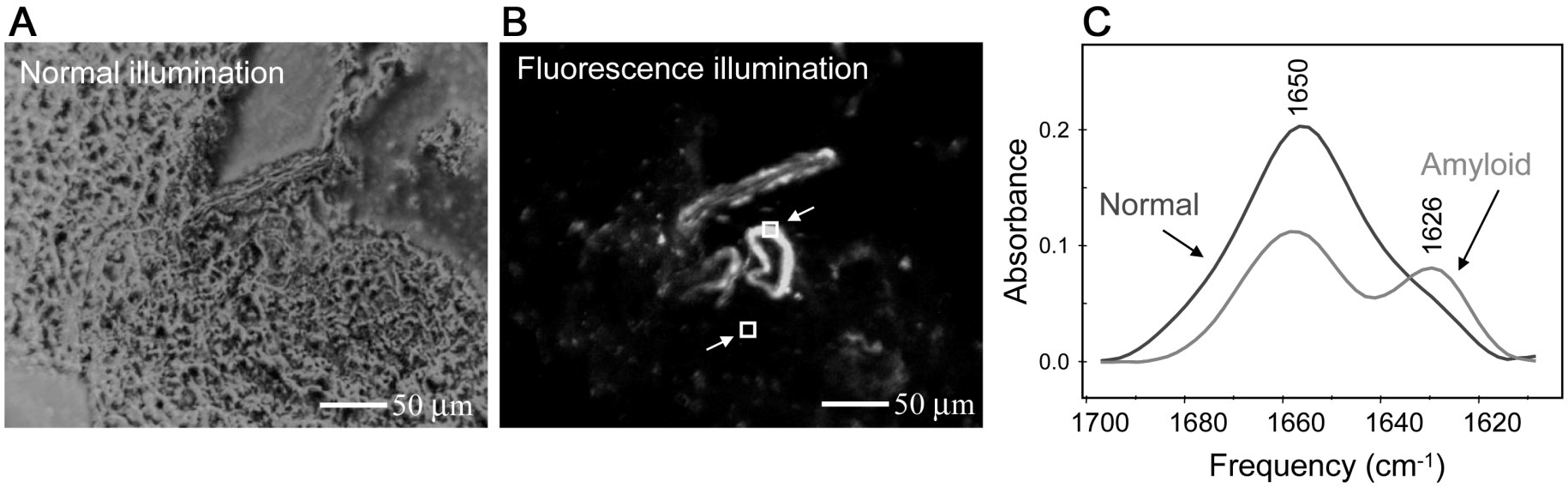

L.M. Miller et al Figure 2

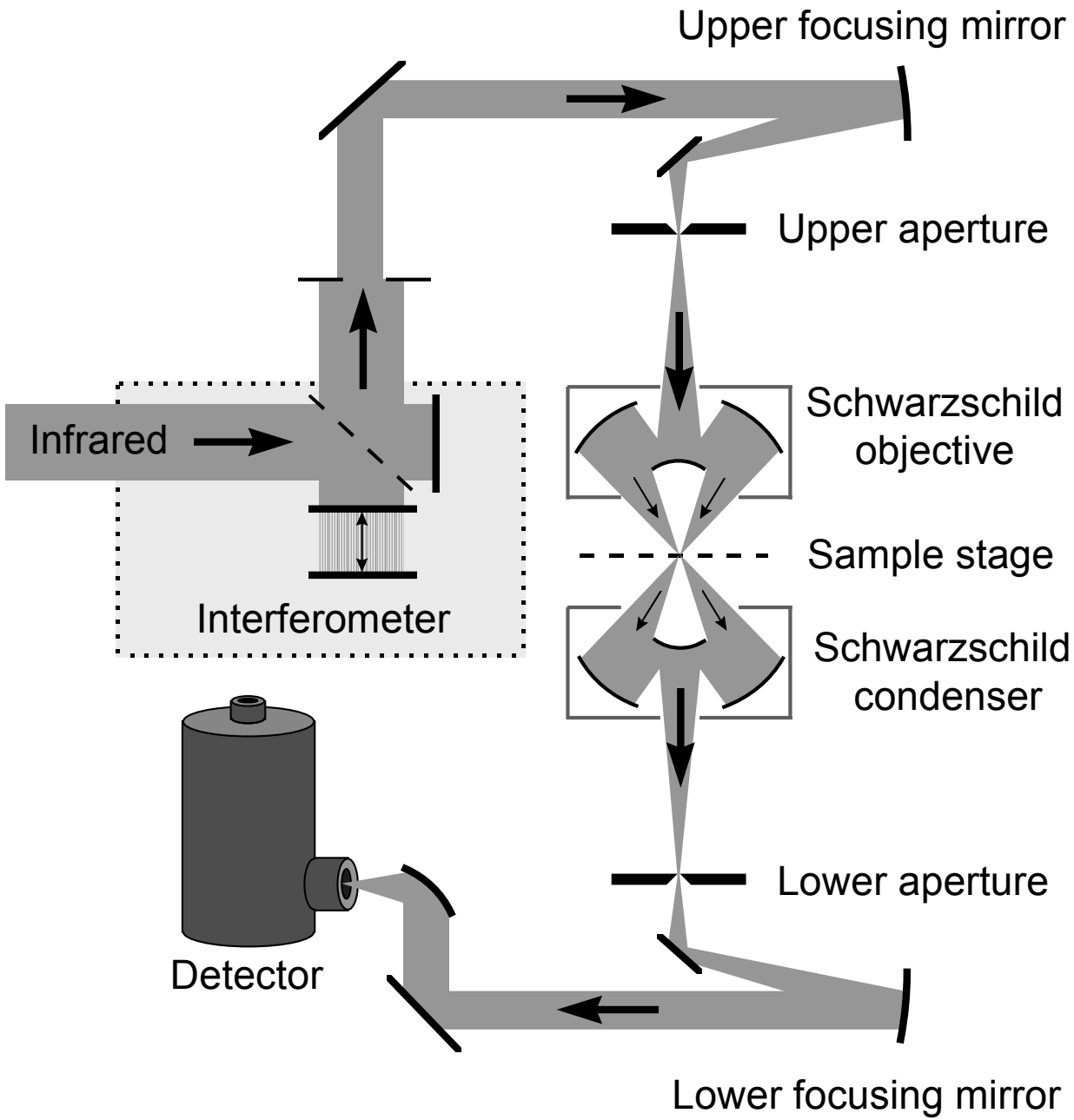

L.M. Miller et al Figure 3

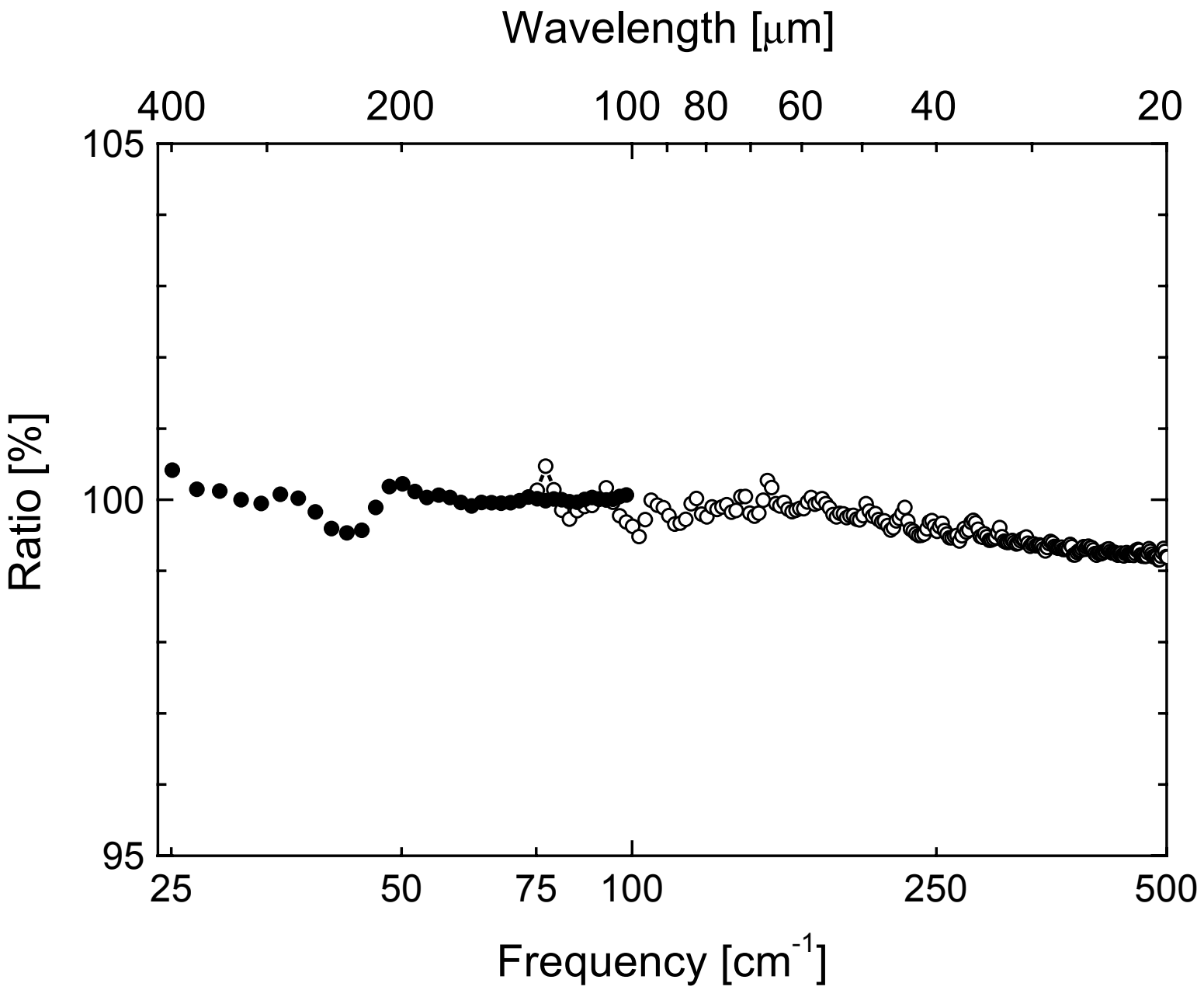

L.M. Miller et al Figure 4

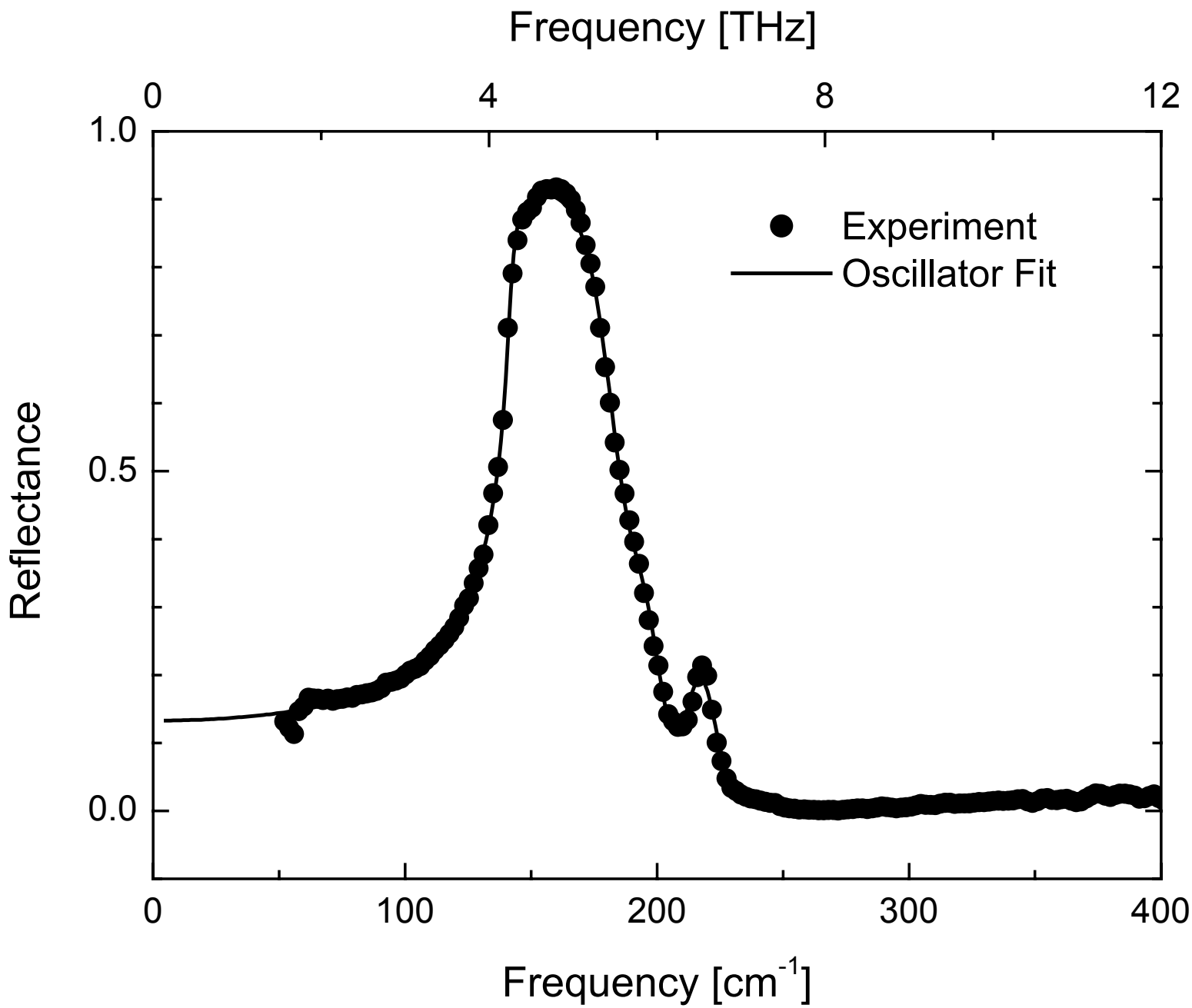

L.M. Miller et al Figure 5

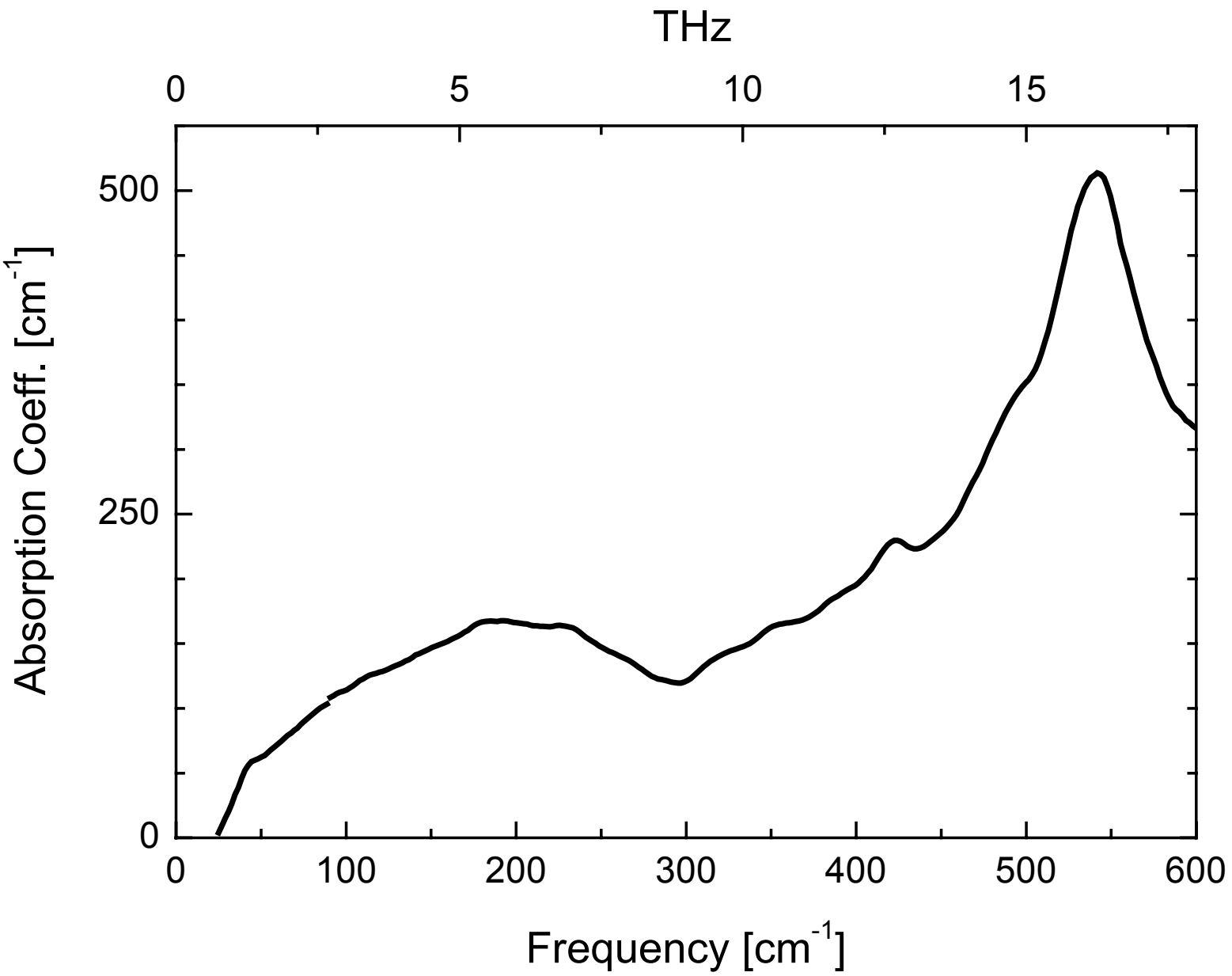

L.M. Miller et al Figure 6